Coverage and Connectivity Aware Energy Charging Mechanism Using Mobile Charger for WRSNs

Yuanping Kan, Chih-Yung Chang, *Member, IEEE*, Chin-Hwa Kuo, and Diptendu Sinha Roy

***Abstract*—Wireless recharging using a mobile charger has been widely discussed in recent years. Most of them considered that all sensors were equally important and aimed to maximize the number of recharged sensors. The purpose of energy recharging is to extend the lifetime of sensors whose major work is to maximize the surveillance quality. In a randomly deployed wireless rechargeable sensor network, the surveillance quality highly depends on the contributions of coverage and network connectivity of each sensor. Instead of considering maximizing the number of recharged sensors, this article further takes into consideration the contributions of coverage and network connectivity of each sensor when making the decision of recharging schedule, aiming to maximize the surveillance quality and improve the number of data collected from sensors to the sink node. This article proposes an energy recharging mechanism, called an energy recharging mechanism for maximizing the surveillance quality of a given WRSNs (ERSQ), which partitions the monitoring region into several equal-sized grids and considers the important factors, including coverage contribution, network connectivity contribution, the remaining energy as well as the path length cost of each grid, aiming to maximize surveillance quality for a given wireless sensor network. Performance studies reveal that the proposed ERSQ outperforms existing recharging mechanisms in terms of the coverage, the number of working sensors as well as the effectiveness index of working sensors.**

***Index Terms*—Connectivity, coverage, mobile charger, recharging, wireless sensor networks (WSNs).**

I. Introduction

WIRELESS sensor networks (WSNs), which consist of many small sensors, play an important role in many monitoring applications, including environmental monitoring, smart home, precision agriculture structural, health monitoring, etc. [1], [2]. Since most of the sensors are mainly powered by the limited capacity of batteries, the lifetime of WSNs is limited, which obstructs the large-scale deployment of WSNs. To prolong the lifetime of WSNs, extensive efforts for energy harvesting have been taken in recent years [3]–[6]. However, the instability of the energy from the environment such as solar and wind results in the WSNs becoming unstable. Therefore, it is very crucial to find a stable energy source to recharge the sensors for maintaining the perpetual operations of WSNs [5], [6].

Manuscript received 27 January 2021; revised 19 May 2021 and 26 July 2021; accepted 27 August 2021. Date of publication 23 September 2021; date of current version 26 August 2022. *(Corresponding author: Chin-Hwa Kuo.)*

Yuanping Kan is with the Fujian Polytechnic Normal University, Fujian 350117, China, and also with the Tamkang University, New Taipei 25137, Taiwan (e-mail: done0250@126.com).

Chih-Yung Chang and Chin-Hwa Kuo are with the Tamkang University, New Taipei 25137, Taiwan (e-mail: cychang@mail.tku.edu.tw; chinhwakuo@mail.tku.edu.tw).

Diptendu Sinha Roy is with the National Institute of Technology, Meghalaya, Shillong 793003, India (e-mail: diptendu.sr@nitm.ac.in).

Digital Object Identifier 10.1109/JSYST.2021.3109056

Wireless energy transferring as a revolutionized energy supply technology provides an alternative solution to prolong the lifetime of the WSNs [7]–[10]. Unlike sensor energy replenishments through energy harvesting, the wireless energy transferring technique is a promising technique to enable wirelessly transfer power with steady and high recharging rates. The state-of-the-art methods employ a mobile charger to charge the sensor nodes in the network when they are within the limited charging ranges of the mobile charger.

In literature, a lot of studies have been proposed for rechargeable WSNs. The key idea of the proposed recharge algorithms is to construct the path and determine the stop points for the mobile charger to recharge the energy of the sensor nodes. These studies can be further classified into two classes: the nonpartition class [11]–[13] and the partitioning class [14]–[16]. Some existing studies [11]–[13] fallen in the nonpartition class mainly required a mobile charger to visit the low-energy sensors to perform the charging task. These algorithms mainly considered the cost of path length, aiming to recharge as many as possible sensors. However, one major challenge is that there are infinite numbers of points where the mobile charger should consider as the stop points for recharging. To cope with this problem, some other studies [14]–[16] partitioned the monitoring region of the WSNs into grids, aiming to simplify the problems of path construction and stop location decisions. These studies took a grid as a basic unit and planed the recharging path according to the number of requested sensors fallen in each grid. However, most of them considered that all sensors are equally important [11], [12], [14], [16].

In a dense WSN, the random deployment might result in a situation in which neighboring sensors might have different sizes of the overlapped region. Fig. 1(a) gives an example that the coverage areas of sensors s_1 and s_2 have a large overlapped region. In this case, even the energy of the sensor s_1 is exhausted, sensor s_2 can still monitor the region and maintain a good monitoring quality. However, as shown in Fig. 1(b), the coverage areas of sensors s_3 and s_4 are not overlapped with each other. In case that the energy of the sensor s_3 was exhausted, the monitoring quality will be reduced since no sensor can monitor the covered region of the sensor s_3. Therefore, the importance of sensors s_3 and s_4 is higher than that of sensors s_1 and s_2 in terms of coverage contribution.

The coverage and connectivity contributions of different sensors are different. The sensor that has the largest coverage

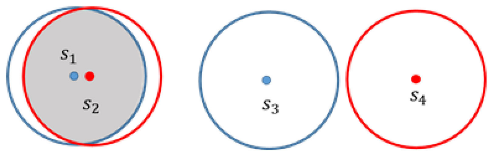

Fig. 1. Example of the different importance of sensors in terms of coverage contribution.

contribution should have the highest priority to be recharged. In addition to the coverage contribution, the connectivity contribution is another important parameter that should be considered when the mobile charger determines the stop points. This occurs because that the sensors closer to the sink node will be responsible for forwarding the data from the other sensors, which are far away from the sink node. In case that these sensors run out of their energies, the network connectivity will be broken, which highly impacts the data collection.

This article aims to maximize the surveillance quality by developing the recharging mechanism, which takes into consideration the coverage and network connectivity contributions. The proposed recharging mechanism, called an energy recharging mechanism for maximizing the surveillance quality of a given WRSNs (ERSQ) algorithm, initially partitions the monitoring region into several equal-sized grids. Then, it schedules the grids to be visited and all sensors fallen in the visited grids will be recharged. To maximize the surveillance quality, the sensors, which have sent the recharging requests will be evaluated against their coverage and network connectivity contributions. Each grid will be assigned a weight according to the evaluation. Based on the weight of each grid and the cost of path length, the mobile charger selects some grids to be visited and then constructs a path passing through these grids.

The main contributions of this article are listed as follows.

1) *Connectivity Awareness:* Connectivity plays an important role since the sensing data cannot be forwarded to the sink node when the network is disconnected, even though a big coverage area is achieved. To our knowledge, previous charging algorithms did not take into consideration the connectivity issue. The proposed ERSQ algorithm further considers the connectivity contribution of the sensors. The mobile charger will recharge the sensors with higher connectivity contributions. Compared to the existing studies [11], [15], the ERSQ algorithm maintains better network connectivity and allows the sink node to collect more data.
2) *Coverage Awareness:* Most existing charging algorithms considered the movement cost and the number of recharged sensors. However, each sensor has different importance depending on its contribution in coverage. Compared with existing studies [11], [15], the proposed ERSQ algorithm takes into consideration the coverage contribution. The mobile charger will recharge the sensor with a higher coverage contribution. As a result, the proposed ERSQ can achieve better coverage, as compared with related studies [11] and [15].
3) *Grid-Based Network Management:* A WSN usually contains a large number of sensors. This article partitions the monitoring region into several regular hexagon grids and the coverage and connectivity of each grid are measured. This can reduce the coverage and connectivity calculations and simplify the path construction.

The rest of this article is organized as follows. Section II summarizes related work. Section III formalizes the assumptions and problem statement. Section IV presents the proposed ERSQ algorithm in detail. Section V further reveals the experimental study and compares the performance of the proposed ERSQ algorithm against the related studies. Finally, Section VI concludes this article.

II. Related Work

In literature, previous studies that adopted a mobile charger to develop recharging mechanisms can be mainly divided into two classes: the nonpartition and partition categories.

A. Nonpartition Model

Some existing studies have fallen into the nonpartition category. Yu *et al.* [11] adopted the mobile charger aiming to prolong the network lifetime. When the energy is smaller than a predefined threshold, the sensor sent a recharging request to the mobile charger. The mobile charger initially constructed a path passing through all the requested sensors. Then, a path reduction algorithm was proposed to reduce the path length.

Zhu *et al.* [12] considered a set of sensors that were required to be recharged. The mobile charger then selected sensors, one by one as the candidate to be recharged and calculates the delay to recharge each sensor. Tu *et al.* [13] constructed a graph $G = (V, E, w)$, where V is the set of sensors needed to be recharged, E is the edge between sensors, w is the weight of each sensor, which is a function considering both the remaining energy of that sensor and the distance between sensors. Then, a charging path is constructed by the mobile charger based on solving the traveling salesman problem. Though the above-mentioned studies [11]–[13] aimed to reduce the path length of the mobile charger, they did not consider the coverage and connectivity issues.

B. Partition Model

In the partition category, the monitoring region is divided into some grids. Then, the recharging demand of sensors in each grid can be treated as the grid demand. As a result, the mobile charger established the path based on the demands of the girds.

Liu *et al.* [14] partitioned the monitoring region into several square grids. The grid, which contained sensors with low-level energy, will be included in the recharging candidate set. The central point of each grid was the charging position for the recharging candidate set. Then, the mobile charger constructed the path based on the number of sensors in the grid.

Tian *et al.* [15] partitioned the monitoring region into some equal-sized hexagon grids. The grid containing sensors is considered as the charging candidate set. In each candidate set, each sensor is labeled with one of three different levels, according to its remaining energy. The mobile charger calculated the charging weight for each grid, according to the level labeled on each sensor in that grid. The grid with the largest charging weight has the highest priority to be recharged by the mobile charger.

TABLE I
COMPARISON BETWEEN ALGORITHMS

	Partitioned Networks	Online Scheduling	Considering Coverage	Considering Connectivity
YCC [11]	×	×	×	×
ZYLL [12]	×	○	×	×
TXYC [13]	×	×	×	×
LNPL [14]	○	×	×	×
TJLM [15]	○	×	×	×
AWA [16]	○	×	×	×
Proposed ERSQ	○	○	○	○

○ = considered, × = not considered.

Alkhalidi *et al.* [16] partitioned the monitoring region into some rings. Each ring was further partitioned into several sectors. The sector with the largest number of recharging requests will be first recharged.

However, most of the existing studies fallen in the partitioned model only considered the number of requested sensors in the grid. Compared with these studies, the proposed ERSQ algorithm further considers the coverage contribution and network connectivity contribution of each sensor. Table I summarizes the comparisons of the related studies and the proposed ERSQ.

III. ASSUMPTIONS AND PROBLEM STATEMENT

This section initially introduces the network model and assumptions of wireless rechargeable sensor networks. Then, the important properties of sensors and the problem formulation of our study are described.

A. Network Environment

Given a rectangle region *R*, this article considers a certain rechargeable WSN, which comprises a set of p static sensors $S = \{s_1, s_2, \ldots, s_p\}$ distributed over a given monitoring region *R*. A sink node, denoted by BS, is deployed at the location of the central point of *R*. The location of *BS* is also called home location. Each sensor is battery powered and its battery is rechargeable by a mobile charger. A mobile charger moves in *R* aiming to charge sensors for maintaining the quality of coverage. This article assumes that the mobile charger has detection software/hardware to cope with the malfunction of the mobile charger. Meanwhile, this article assumes that there is at least one standby mobile charger at the base station. As soon as the working mobile charger detects the malfunction, it will send an emergent request to the base station, which will notify the standby one to take over the recharging task.

A cycle *T* is the duration in which the mobile charger leaves BS, moves and recharges some sensors, and finally goes back to *BS*. Herein, it is assumed that the mobile charger has rich energy for executing the scheduling, moving, and recharging tasks in one cycle. The recharge scheduling aims to obtain the best surveillance quality in one cycle *T*.

Let r_s and r_c denote the sensing radius and communication radius of each sensor, respectively. Assume that each sensor s_i is aware of its location (x_i, y_i). Assume that the mobile charger knows its location and the locations of all sensor nodes. Let $d_{i,j}$ denote the distance between the sensors s_i and s_j. Similarly, let $d_{i,car}$ denote the distance between the mobile charger and sensor s_i. The following presents the energy model considered in this article.

B. Energy Model

Let E denote the initial energy of each sensor and $E_{\min}$ denotes the energy threshold below, which the sensor should not work and switch to the sleep state. Assume that each packet contains k bits. Let E_s denote the energy consumption for sensing in each time unit. Let E_R and E_T denote the energy consumptions for receiving and transmitting one packet (k bits), respectively. Consider the communication pair s_i and s_j , which play the roles of the sender and receiver, respectively. The energy consumption of s_j for receiving one packet can be measured by $E_R = k{*}p_r$, where p_r is the energy consumption per bit incurred by the receiving circuit. On the other hand, the energy consumption for the sender s_i to transmit one packet is measured by $E_T = k * \varepsilon_1 + k * d_{i,j}^{pl} * \varepsilon_2$, where ε_1 is a factor that represents the energy consumption per bit of transmitting circuit, ε_2 is the energy consumption per bit of the amplifier circuit, and pl is the path-loss exponent, which typically ranges between 2 and 4, depending on the environment [17].

Assume that the observing time T is partitioned into q equal time slots $t_1, t_2, \ldots, t_q$. Let τ denote the length of each time slot. That is, $\tau = T/q$. Let $E_{i,t}^{rem}$ denote the remaining energy of the sensor s_i at time slot t.

Let Boolean variable $\lambda_{i,t}$ denote whether or not $E_{i,t}^{rem}$ of sensor s_i is more than $E_{\min}$ at time slot t

$$\lambda_{i,t} = \begin{cases} 1 & E_{i,t}^{rem} > E_{\min} \\ 0 & \text{otherwise.} \end{cases} \tag{1}$$

Let Boolean variable $\mu_{i,t}$ denote the connectivity between sensor s_i and BS at time slot t. That is

$$\mu_{i,t} = \begin{cases} 1 & s_i \text{ and } BS \text{ is connected} \\ 0 & \text{otherwise.} \end{cases} \tag{2}$$

The coverage of WSNs at time t can be measured by applying

$$C_{\text{net}}^t = \bigcup\nolimits_{s_i \in S} \lambda_{i,t} * \mu_{i,t} * \Omega_{\ s_i} \tag{3}$$

where Ω_s is the coverage of any sensor s.

Let $E_{i,t}^c$ denote the recharged energy obtained by the sensor s_i at time slot *t*. Let $E_{i,j}^s$, $E_{i,j}^R$, and $E_{i,j}^T$ denote the energy consumptions for sensor s_i performing operations of sensing, receiving, and transmitting in the jth slot, respectively. Let Boolean variable $\rho_{i,t}$ denote whether or not s_i is charged at time slot t. That is

$$\rho_{i,t} = \begin{cases} 1 & s_i \text{ is charged in slot } t \\ 0 & \text{otherwise.} \end{cases} \tag{4}$$

Assume that the network starts running at the time point t_{start}. At time slot t, the remaining energy of the sensor s_i can be calculated by [17]

$$E_{i,t}^{rem} = E - \sum_{t_j = t_{\text{start}}}^{t} \left(E_{i,j}^s + E_{i,j}^R + E_{i,j}^T - \rho_{i,t_j} * E_{i,t}^c \right). \tag{5}$$

Based on the above-mentioned energy model, the objective of this article is presented below.

C. Objective

The major goal of this article is to maximize the surveillance quality of the monitoring region. This can be achieved by maximizing the accumulated coverage at any given time. The following presents the objective of this article.

Objective: In period T, the WSN network cumulative maximum coverage is

$$\mathbf{Max}\left(\sum_{t\,=\,t_{\text{start}}}^{T+t_{\text{start}}} C_{\text{net}}^{t}\right). \tag{6}$$

D. Constraints

When achieving the above-mentioned objectives, some constraints should be satisfied.

Let Boolean variable $\varphi_{i,t}^{\text{work}}$ denote the state of the sensor s_i. Since each sensor stays in either work or sleep state, we have

$$\varphi_{i,t}^{\text{work}} = \begin{cases} 1 & s_i \text{ stays in the work state at time slot } t \\ 0 & \text{otherwise.} \end{cases} \tag{7}$$

Similarly, let $\varphi_{i,t}^{\text{sleep}}$ denote whether or not the sensor s_i stays in the sleep state. That is

$$\varphi_{i,t}^{\text{sleep}} = \begin{cases} 1 & s_i \text{ stays in the sleep state at time slot } t \\ 0 & \text{otherwise.} \end{cases} \tag{8}$$

Each sensor should satisfy the sensor state constraint. That is, each sensor can stay in either the work state or the sleep state. In other words, no sensor can stay in work and sleep states simultaneously.

1) Sensor State Constraint: At time slot t, each sensor should satisfy the constraint

$$\varphi_{i,t}^{\text{work}} + \varphi_{i,t}^{\text{sleep}} = 1. \tag{9}$$

In addition to the sensor state constraint, the following presents the minimal remaining energy constraint, which asks each sensor to reserve minimal energy for basic operation and state switching. Recall that $\lambda_{i,t}$ denotes whether or not the remaining energy $E_{i,t}^{rem}$ of sensor s_i is more than $E_{\min}$ at time slot t.

2) Minimal Energy Constraint: Each sensor can stay in the work state if its remaining energy is not smaller than $E_{\min}$

$$\lambda_{i,t} + \varphi_{i,t}^{\text{sleep}} = 1. \tag{10}$$

Another constraint specifies the upper bound of the recharged energy of each sensor. Let P_{car} and P_{s_i} denote the transmitted and received power of the mobile charger and sensor s_i, respectively. According to the energy charging model proposed in [11], [18], and [19], (11) presents the recharged energy of the sensor s_i

$$P_{s_i} = \begin{cases} \frac{P_{car}G_rG_tr_w^2}{(4\pi d_{i,car})^2 f} & d_{i,car} < \frac{4\pi\sqrt{f}h_th_r}{\lambda} \\ \frac{P_{car}G_rG_t(h_th_r)^2}{(d_{i,car})^4} & d_{i,car} > \frac{4\pi\sqrt{f}h_th_r}{\lambda} \end{cases} \tag{11}$$

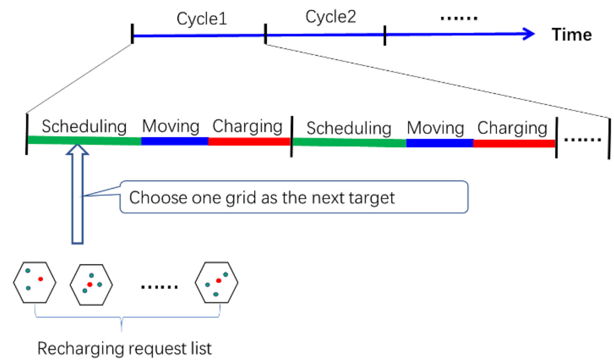

Fig. 2. Cycle T consists of several rounds, each of which consists of three tasks. In the scheduling task, the proposed ERSQ algorithm is applied.

where G_t denotes the gain of transmitting antenna of the mobile charger, G_r denotes the gain of receiving antenna of the sensor s_i, r_w denotes the carrier wavelength, f refers to the system loss factor, $d_{i,car}$ denotes the propagation distance between antennas, h_t and h_r denote the height of the transmitting and receiving antenna above ground, respectively. Let r_{car} denote the radius of the charging range of the mobile charger. To obtain the energy from the mobile charger, sensor s_i should fall in the recharge range of the mobile charger. That is, $d_{i,car}$ must be smaller than r_{car}. Hence, the lower bound of the P_{s_i} is,

$$\frac{P_{car}G_rG_t(h_th_r)^2}{(r_{car})^4}. \tag{12}$$

The recharge energy of the sensor s_i also has an upper bound, which should be smaller than the transmitted power of the mobile charger. The following recharged energy constraint reflects the lower and upper bounds of the recharged energy of each sensor s_i.

3) *Recharged Energy Constraint:*

$$\frac{P_{car}G_rG_t(h_th_r)^2}{(r_{car})^4} \le P_{s_i} \le P_{car}. \tag{13}$$

IV. Proposed ERSQ Algorithm

The observed cycle T consists of several rounds, as shown in Fig. 2. In each round, three tasks are performed, including scheduling, moving, and recharging. In the first task, the mobile charger schedules the recharging path based on the proposed ERSQ algorithm, which consists of two phases. Then, the mobile charger performs the moving task, aiming to move from the current location to the next recharging grid. After that, the mobile charger performs the recharging task, aiming to recharge all the sensors in the target grid. The three tasks will be performed round by round during the observed period T.

The proposed ERSQ algorithm aims to maximize the surveillance quality of the given monitoring region R. It mainly consists of two phases. First, the *initial phase* aims to partition the monitoring region into some regular hexagon grids and establish the coordinate system for the grids. Then, the *coverage-based benefit evaluation* (CBBE) *phase* aims to calculate the benefit of each hexagon grid based on its coverage improvement. After

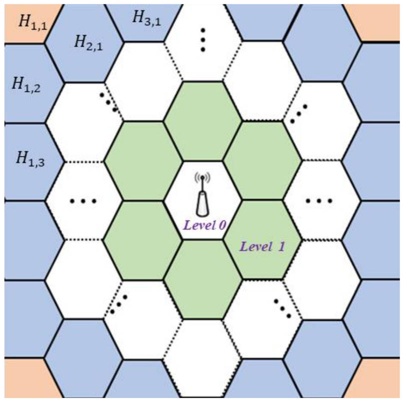

Fig. 3. Partition of the monitoring region *R*.

that, the CBBE phase further selects a target hexagon grid which obtains the maximal benefit. This also reflects the goal given in (6). The following presents the details of each phase.

A. Initial Phase

This phase aims to partition the monitoring region into some regular hexagon grids. The motivation for region partition is illustrated below. The key idea of the proposed ERSQ algorithm is to construct the path and determine the stop points for the mobile charger to recharge the static sensors such that the coverage quality provided by the sensors can be maximized. However, one major challenge is that there are infinite numbers of points where the mobile charger should consider as the stop points. To cope with this problem, the monitoring region R will be partitioned into some equal-sized regular hexagon grids. The size of each grid can impact the charging performance of a given WSN. In case that the grid size is big, each grid will contain many sensors. An additional algorithm should be developed to determine the locations for a mobile charger to perform the charging task. On the contrary, a small grid might increase the computational complexity when developing the charging algorithm. In this article, it is assumed that the radius of the mobile charger is the length of the regular hexagon edge. That is, the charging range of the mobile charger can cover the whole regular hexagon. As a result, the mobile charger only needs to determine some center points of the hexagon grids as the candidates of the stop points. In the performance study, the grid size will be a parameter whose value will be varied to investigate its impact on performance.

Let N_A denote the number of hexagon grids in region R. As shown in Fig. 3, the most top-left grid in R is labeled with coordinates $(1, 1)$. The x coordinate and y coordinate are increased by one if the location of a grid shifts one position toward the right and down directions, respectively. Let $H_{m,n}$ denote the grid with coordinates $(m,\ n)$. Let (x_m, y_n) and $S_{m,n}$ denote the center location of $H_{m,n}$ and the set of sensors in $H_{m,n}$, respectively. Let $(x_{\text{center}},\ y_{\text{center}})$ denote the center point of R. Let H_{center} denote the center hexagon grid, which contains the center point $(x_{\text{center}},\ y_{\text{center}})$. Let BS denote the static sink node which is deployed at the location $(x_{\text{center}},\ y_{\text{center}})$.

All the sensors $s_i \in S_{m,n}$ can form a cluster in each hexagon grid $H_{m,n}$. Initially, the sensor $s_i \in S_{m,n}$ closest to the center location (x_m, y_n) will play the role of anchor, called $a_{m,n}$ of the grid $H_{m,n}$. The anchor $a_{m,n}$ is responsible for receiving the sensing data from $s_i \in S_{m,n}$ and then forwarding them along the path from the current hexagon grid to BS. To balance the energy consumptions of sensors in one hexagon grid, all sensors in the same hexagon grid will act as the anchor in turn.

B. CBBE Phase

This phase aims to calculate the benefit of each hexagon grid based on the coverage of working sensors in that grid. The motivation for calculating the hexagon grid benefit is illustrated below. The recharging operation of the mobile charger is executed grid by grid. That is, the mobile charger will select the grid, which can contribute the largest benefit in terms of coverage as the target grid for performing the recharging task. Therefore, evaluating the coverage benefit of each grid is important.

The coverage contribution of each grid is the overall coverage contributed by the sensors in that grid. The coverage ranges of several sensors in the same grid might be overlapped. This indicates that the coverage of one certain area might be contributed by more than one sensor. To accurately measure the coverage benefit of each hexagon grid, the following defines *independent coverage contribution* of each hexagon grid $H_{m,n}$, denoted by $B^{\text{coverage}}_{m,n}$, which represents the area of hexagon grid $H_{m,n}$ covered by working sensors $s_i \in S_{m,n}$.

Let Q denote a set of sensors. Let Ω_Q denote the overall coverage area contributed by sensors $s_i \in Q$. Let $A_{m,n}$ denote the area of hexagon grid $H_{m,n}$. The *independent coverage contribution* $B^{\text{coverage}}_{m,n}$ of $S_{m,n}$ can be calculated by applying

$$B^{\text{coverage}}_{m,n} = \Omega_{S_{m,n}} \cap A_{m,n}. \tag{14}$$

That is, the independent coverage contribution of hexagon grid $H_{m,n}$ only counts for those areas, which are the overall coverage area of $s_i \in S_{m,n}$ in area $A_{m,n}$.

When the mobile charger calculates the benefit of a hexagon grid, it considers many parameters. In addition to the coverage benefit, the connectivity contribution of one hexagon grid is another important parameter that should be taken into consideration. The data in each hexagon grid $H_{m,n}$ is transmitted along a path, say $P_{m,n}$, from anchor $a_{m,n}$ to BS, as shown in Fig. 3. Let $H_{i,j}$ is one hexagon grid passed through by path $P_{m,n}$. Since $H_{i,j}$ is closer to the *BS* than $H_{m,n}$, the failure of $s_k \in S_{i,j}$ might block the transmission of path $P_{m,n}$. This implies that the hexagon grid $H_{i,j}$ is more important than $H_{m,n}$ in terms of connectivity. Therefore, the hexagon grid $H_{i,j}$ closer to the BS should have a larger benefit than the other hexagon grids. To prevent WSNs from disconnection, the mobile charger should charge the sensors in the hexagon grid closer to the *BS*. To distinguish the benefits of closer grids and farther grids, the following introduces the concept of *level,* which helps calculate the connectivity benefit of each hexagon grid.

Fig. 3 shows a partitioned region *R*. The central hexagon grid will be treated as *level 0* and is marked with white color. The hexagon grids, which neighbor the central hexagon grid have formed a ring of six hexagon grids. These hexagon grids will be considered as *level 1* and are marked with green color. Similarly, the hexagon grids which are neighbors to the hexagon grids of *level 1* will form another ring and be considered as *level 2*. All hexagon grids will be labeled with a level number and marked with different colors, depending on its the level number is even or odd, respectively.

Let Φ^k denote the set of hexagon grids labeled with level k and $|\Phi^k|$ denotes the number of elements in Φ^k. Let $k_{\max}$ denote the maximum value of k. The following further defines the *connectivity index* of a hexagon grid $H_{m,n} \in \Phi^k$, which indicates the average number of hexagon grids whose transmission path passing through $H_{m,n}$. Let $B_{m,n}^{\text{connect}}$ denote the *connectivity benefit* of hexagon grid $H_{m,n}$, which can be calculated by applying

$$B_{m,n}^{\text{connect}} = \frac{\sum_{i=k+1}^{k_{\max}} |\Phi^i|}{|\Phi^k|}. \quad (15)$$

Let $B_{m,n}$ denote the charging benefit of $H_{m,n}$ at some time t. It can be calculated by applying

$$B_{m,n} = \alpha \left(B_{m,n}^{\text{coverage}}\right) + (1-\alpha) B_{m,n}^{\text{connect}} \quad (16)$$

where $\alpha \in [0,1]$ determines the weights of $B_{m,n}^{\text{coverage}}$ and $B_{m,n}^{\text{connect}}$. Since it takes time to go to $H_{m,n}$ and charge the sensors in $H_{m,n}$, all the sensors outside the hexagon grid $H_{m,n}$ will consume their energy. As a result, some sensors may exhaust their energies during the execution of the charging task performed for the hexagon grid $H_{m,n}$, leading to the problems of connectivity and coverage losses.

Let H_{curr} denote the hexagon grid in which the mobile charger falls at the time t. Let $t_{curr \to m,n}^{\text{travel}}$ and $t_{m,n}^{\text{charge}}$ denote the times required to move to $H_{m,n}$ and the time required for charging the sensors in $H_{m,n}$, respectively. Let $T_{m,n}$ denote the total time required for the execution of the charging process for $H_{m,n}$. We have

$$T_{m,n} = t_{curr \to m,n}^{\text{travel}} + t_{m,n}^{\text{charge}}. \quad (17)$$

The following presents the total loss of benefits when the mobile changer moves from the current grid to grid $H_{m,n}$, which consists of connectivity loss and coverage loss. First, the connectivity loss will be discussed. Let Boolean variable $\psi_{i,j}$ denote whether or not the hexagon grid $H_{i,j}$ is connected to the *BS* in the time interval $[t, t+T_{m,n}]$. We have

$$\psi_{i,j} = \begin{cases} 1 & H_{i,j} \text{ is connected in } [t, t+T_{m,n}] \\ 0 & \text{otherwise.} \end{cases} \quad (18)$$

In particular, $\psi_{i,j} = 0$ indicates that the connectivity benefit of $H_{i,j}$ will be lost in the time interval $[t, t+T_{m,n}]$. Let $L_{m,n}^{\text{connect}}$ denote the connectivity loss during $[t, t+T_{m,n}]$. Equation (19) calculates the value of $L_{m,n}^{\text{connect}}$

$$L_{m,n}^{\text{connect}} = \sum_{k=1}^{k_{\max}} \left(\sum_{H_{i,j} \in \Phi^k} (1-\psi_{i,j}) B_{i,j}^{\text{connect}} \right). \quad (19)$$

In addition to the connectivity loss, the following further considers the coverage loss. Herein, it is noticed that the coverage loss might be raised due to two reasons. One is the working sensor unable to deliver its sensing information to the *BS* and the other is the sensor sleeping. First, the sensor unable to deliver its sensing information will be considered. Let Boolean variable $\varphi_{i,t}$ denote the state of the sensor s_i in the time interval $[t,\ t+T_{m,n}]$. Since each sensor stays in either work or sleep states, we have

$$\varphi_{i,\hat{t}} = \begin{cases} 1 & s_i \text{ in the work state for } \hat{t} \in [t,\ t+T_{m,n}] \\ 0 & \text{otherwise.} \end{cases} \quad (20)$$

Let $S_{i,j}^{\text{work}}$ denote the set of working sensors in $H_{i,j}$ in the time interval $[t,\ t+T_{m,n}]$, we have

$$S_{(i,j)}^{\text{work}} = \left\{ s_k | s_k \in S_{(i,j)} \text{ and } \varphi_{k,\hat{t}} = 1, \hat{t} \in [t,\ t+T_{m,n}] \right\}. \quad (21)$$

In case that some sensors are in a disconnected hexagon grid, their sensing information cannot reach the *BS*. As a result, they do not contribute any coverage. This type of coverage loss is called type 1 coverage loss and is denoted by $L_{m,n}^{\text{coverage},1}$. Equation (22) calculates the value of $L_{m,n}^{\text{coverage},1}$

$$L_{m,n}^{\text{coverage},1} = \sum_{k=1}^{k_{\max}} \sum_{H_{i,j} \in \Phi^k} (1-\psi_{i,j}) (\Omega_{S_{i,j}^{\text{work}}} \cap A_{i,j}). \quad (22)$$

Let $L_{m,n}^{\text{coverage},2}$ denote the type 2 coverage loss, which occurs due to the sleeping sensors in the connected hexagon grids. The value of $L_{m,n}^{\text{coverage},2}$ can be calculated by applying

$$L_{m,n}^{\text{coverage},2} = \sum_{k=1}^{k_{\max}} \sum_{H_{i,j} \in \Phi^k} \psi_{i,j} [A_{i,j} - (\Omega_{S_{i,j}^{\text{work}}} \cap A_{i,j})]. \quad (23)$$

Let $L_{m,n}$ denote the total coverage loss, which consists of the connectivity loss and type 1 and type 2 coverage losses. The value of $L_{m,n}$ can be measured by applying

$$L_{m,n} = \beta L_{m,n}^{\text{connect}} + \gamma L_{m,n}^{\text{coverage},1} + (1-\beta-\gamma) L_{m,n}^{\text{coverage},2} \quad (24)$$

where $\beta, \gamma \in [0,1]$ are the weights of the three types of loss.

Let $W_{m,n}$ denote the benefit of the $H_{m,n}$ to the coverage of WSNs, which is recharged at time t. Equation (25) measures the value of $W_{m,n}$

$$W_{m,n} = B_{m,n} - L_{m,n}. \quad (25)$$

The recharging policy is to select one grid that needs to be recharged and obtains the maximal benefit. That is, the mobile charger will move to the hexagon grid H^{best} if it satisfies

$$H^{\text{best}} = arg \operatorname*{Max}_{H_{m,n}} W_{m,n}. \quad (26)$$

The following summarizes the ERSQ algorithm, as shown in Fig 4.

The proposed ERSQ algorithm can be summarized as follows.

1) The monitoring region is partitioned into some regular hexagon grids to simplify the calculation.
2) The grids are grouped into different levels according to the distance from the sink to calculate the connectivity of the grids.

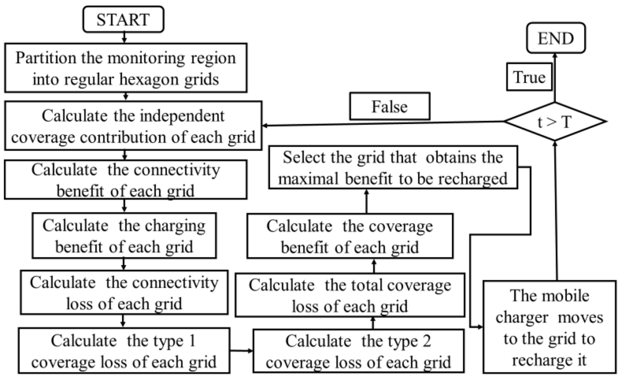

(a)

Algorithm: *ERSQ*.
Inputs: The location of each sensor $\boldsymbol{s_i}$, the size of the monitoring region and length of hexagon edge.
Output: The recharging path of the mobile charger.

	/* Initialization Phase */
1	Partition the monitoring region into N_A regular hexagon grids $H_{m,n}$,
2	Let $S_{m,n}$ denote the set of sensors in $H_{m,n}$
3	Repeat
	/* Calculation of the charging benefit of each grid*/
4	$B^{coverage}_{m,n} = \Omega_{S_{m,n}} \cap A_{m,n}$
5	$B^{connect}_{m,n} = \frac{\sum_{i=k+1}^{k_{max}} \lvert\Phi^i\rvert}{\lvert\Phi^k\rvert}$
6	$B_{m,n} = \alpha(B^{coverage}_{m,n}) + (1-\alpha)B^{connect}_{m,n}$
	/* The total coverage loss of each grid*/
7	$L^{connect}_{m,n} = \sum_{k=1}^{k_{max}} (\sum_{H_{i,j}\in\Phi^k} (1-\psi_{i,j})B^{connect}_{i,j})$
8	$L^{coverage,1}_{m,n} = \sum_{k=1}^{k_{max}} \sum_{H_{i,j}\in\Phi^k} (1-\psi_{i,j})(\Omega_{S^{work}_{i,j}} \cap A_{i,j})$
9	$L^{coverage,2}_{m,n} = \sum_{k=1}^{k_{max}} \sum_{H_{i,j}\in\Phi^k} \psi_{i,j}[A_{i,j} - (\Omega_{S^{work}_{i,j}} \cap A_{i,j})]$
10	$L_{m,n} = \beta L^{connect}_{m,n} + \gamma L^{coverage,1}_{m,n} + (1-\beta-\gamma)L^{coverage,2}_{m,n}$
	/* Calculate the coverage benefit of each grid */
11	$W_{m,n} = B_{m,n} - L_{m,n}$
	/* Select the best grid which obtains the maximal benefit to be recharged */
12	$H^{best} = \boldsymbol{arg\ Max}_{H_{m,n}} W_{m,n}$
13	The mobile charger moves to H^{best} and recharge it
14	Add H^{best} to the path of the mobile charger
15	Until ($t > T$)

(b)

Fig. 4. ERSQ algorithm. (a) Workflow of the proposed ERSQ. (b) Pseudocode of the proposed ERSQ.

3) For each grid that needs to be recharged at time *t*, its benefit to the surveillance quality of the monitoring region is calculated based on its coverage and network connectivity.
4) The mobile charger selects a grid that obtains the maximal benefit to recharge at time *t*.

According to the ERSQ algorithm, the monitoring region can maintain the maximum surveillance quality at any time *t*. It also reflects the goal given in (3). The following presents the simulation to verify the performance of the ERSQ algorithm compared with [11] and [15] in terms of the accumulated coverage.

TABLE II
SIMULATION PARAMETERS

Parameters	Values
Monitoring region	80m*100m
Number of sensors	50-90
Node deployment	Randomly
Length of the hexagon edge	5m-20m
The sensing range: r_s	5m-20m
Mobile charger speed: v	5 m/s
The energy consumption for moving of the mobile charger: E_{move}	30 J/m
The energy consumption for sensing: E_S	0.05J
The energy consumption for receiving and transmitting: E_T, E_R	0.02J
The transmitted power of the mobile charger: P_{car}	5 J/s
The initial energy of each sensor: E	1000 J

The computational complexity of the proposed algorithm is discussed as follows. Fig. 4 depicts the proposed ERSQ algorithm. In steps 1 and 2, the partition of the whole region into grids requires $O(N_A)$. In the worst case, the complexity of the steps 4–6 are $O((\frac{p}{N_A})^2)$, $O((N_A)^{\frac{1}{2}})$ and $O(1)$, respectively. Therefore, the total complexity of the charging benefit of a grid is $O((\frac{p}{N_A})^2) + O((N_A)^{\frac{1}{2}}) + O(1)$. In general, the number of sensors is much larger than that of grids, so the complexity of the charging benefit of a grid is simplified as $O((\frac{p}{N_A})^2)$. Therefore, the total complexity of the calculation of the charging benefit of each grid is $O(\frac{p}{N_A}^2)$. The complexity of steps 7–10 are $O(N_A)$ $O(N_A)$, $O(N_A)$ and $O(1)$, respectively. The complexity of the total coverage loss of a grid is $3O(N_A) + O(1)$, which can be simplified as $O(N_A)$. Therefore, the total complexity of the total coverage loss of each grid is $O(N_A^2)$. In step 11, the calculation of the coverage benefit of a grid takes constant time leading to the complexity of O(1), so the total complexity of the calculation of the coverage benefit of each grid is $O(N_A)$. In steps 12–14, each step takes constant time leading to the complexity of $O(1)$. Therefore, the complexity of a loop is $O(\frac{p}{N_A}^2) + O(N_A^2) + O(N_A) + 3O(1)$, which can be simplified as $O(\frac{p}{N_A}^2)$. The observing time T is partitioned into q equal time slots, so the number of the loops is most to be q. Finally, the total complexity of the proposed ERSQ algorithm is $O(N_A) + O(\frac{qp}{N_A}^2)$, which can be simplified as $O(\frac{qp}{N_A}^2)$. The total complexity of the [11], [13], and [15] is $O(p^2)$ under the same conditions.

V. SIMULATION

This section investigates the performance of the proposed ERSQ algorithm by comparing it with existing studies, including YCC [11], ZYLS [12], and TJLM [15] algorithms. The parameters used in the experiments of the four algorithms are given in Table II [6], [13].

As shown in Fig. 5, the given region is initially covered by 32 hexagon grids. All sensor nodes are deployed randomly and they can communicate with sensors in the same and the neighbor hexagon grids. Fig. 5 depicts a deployment snapshot of 90 sensor nodes in the region.

The elapsed time is set at 5 units. The length of the hexagon edge is set at 10 m while the sensing range of each sensor is set at 5 m. Fig. 6(a) compares the coverage of the monitoring region by

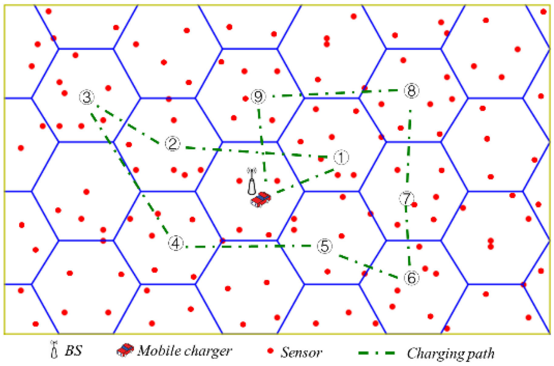

Fig. 5. Simulation environment.

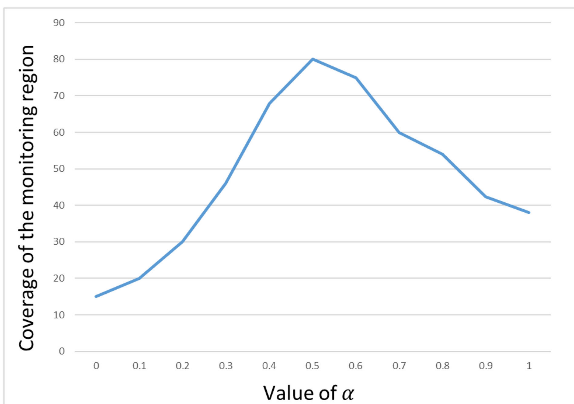

(a)

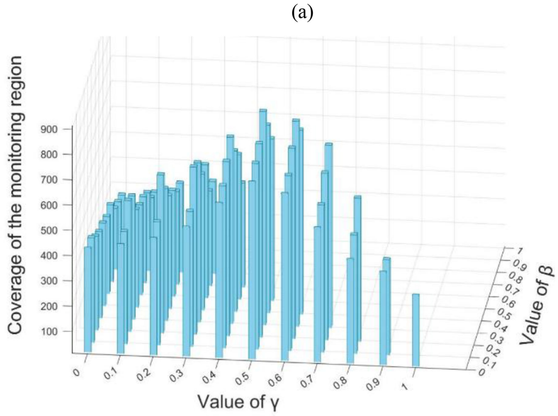

(b)

Fig. 6. Evaluation of parameters in ERSQ algorithm. (a) Influence of α on the coverage of the monitoring region. (b) Influence of β, γ on the coverage of the monitor region.

varying the values of α in the ERSQ algorithm. And the values of β and γ in the ERSQ algorithm are set at 0.4 and 0.2, respectively. As the value of α increases, the coverage of the monitoring region increases to the maximum value and then decreases gradually. This experiment shows that the optimal value of α is 0.5, so the value of α in the following experiments is set at 0.5. Fig. 6(b) compares the coverage of the monitoring region by varying the values of β and γ in the ERSQ algorithm. According to the experiment, when the coverage of the monitoring region reaches the maximum value, the corresponding values of β and γ are 0.3 and 0.5, respectively. Therefore, the values of α , β, and γ are set at 0.5, 0.3, and 0.5 in the following simulation.

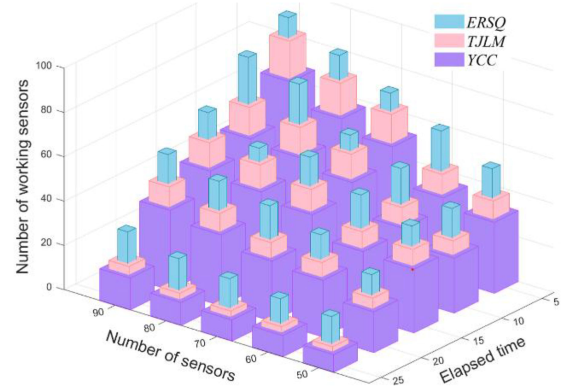

Fig. 7. Comparison of three algorithms in terms of the number of working sensors.

Fig. 7 compares the three algorithms in terms of the number of working sensors by varying the number of sensors ranging from 50 to 90 and the elapsed time ranging from 5 to 25 time units. The length of the hexagon edge is set at 10 m. Herein, a sensor is considered as the working sensor if it works on sensing and its sensing data can be successfully transmitted to the *BS*. In some cases, the sensor will not be considered as a working sensor though it is working. This occurs because that its data cannot be delivered to the *BS* due to the network connectivity problem. A similar trend can be found that the number of working sensors is increased with the number of deployed sensors but is decreased with the elapsed time. This occurs because that a larger number of deployed sensors can support better network connectivity. However, the remaining energy will be reduced with the elapsed time. As a result, the network connectivity will be reduced, especially for those regions closer to the *BS*. In comparison, the proposed ERSQ algorithm outperforms the other two algorithms in terms of the number of working sensors in all cases. This occurs because that the existing YCC and TJLM algorithms only considered the remaining energy and the distance. However, the proposed ERSQ further considers the connectivity issue and precharges the sensors, which might raise the network disconnection problem. As a result, the sensors, which are working on sensing can have more opportunities to deliver their sensing data to the *BS*.

Fig. 8 investigates both the coverage efficiency and sensor efficiency. The coverage and sensor efficiencies are defined by the increased coverage and increased number of sensors per unit path length of the mobile charger, respectively. The simulation environment is the same, as shown in Fig. 7. A common trend of the three algorithms is that both the coverage and sensor efficiencies are increased with the number of deployed sensors. The main reason is that the density of sensors is increased with the number of deployed sensors, increasing the number of recharged sensors per unit path length. In comparison, the performance of the proposed ERSQ algorithm is better than the other algorithms in all cases. This occurs because that the proposed ERSQ algorithm will select the hexagon grid, which

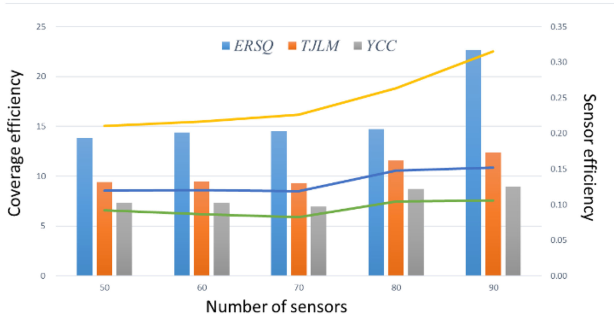

Fig. 8. Comparison of three algorithms in terms of coverage and sensor efficiencies when the number of deployed sensors is varied.

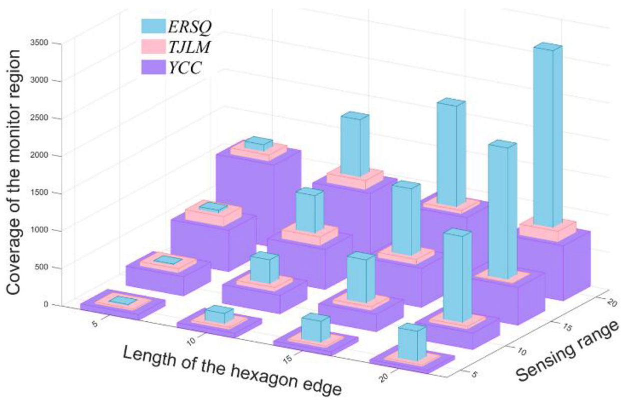

Fig. 9. Comparison of three algorithms in terms of the coverage of the monitoring region.

can have a maximal improvement in terms of coverage and connectivity by considering the movement cost.

Fig. 9 compares the three algorithms in terms of coverage by varying the length of the hexagon edge and the sensing range of sensors. The number of sensors is set at 50 while the elapsed time is set at 50 time units. A common trend of the three algorithms is that their coverages are increased with both the sensing range and the length of the hexagon. When the sensing range of each sensor is increased, its covered area is also increased, which helps increase the coverage contribution. As a result, the coverages of the three algorithms are increased with the sensing range. In addition, the sensor data are forwarded to the *BS* with a fewer number of hops. This occurs because that the number of forwarding layers is decreased if the hexagon edge is increased. As a result, the forwarding cost can be reduced. In comparison, the performance of the proposed ERSQ algorithm is better than those of the other algorithms. This occurs because the proposed ERSQ algorithm takes into consideration the coverage and prior to recharge the one with larger coverage improvement.

Fig. 10 compares the three algorithms in terms of the number of working sensors in a similar environment, as shown in Fig. 9. A common trend of the three algorithms is that the numbers of working sensors are decreased with the sensing range. This occurs because that the energy consumption of the sensor is increased with the sensing range. In comparison, the proposed ERSQ algorithm outperforms the other two algorithms. This occurs because that the proposed ERSQ algorithm considers the connectivity of the sensors. The sensors, which are disconnected

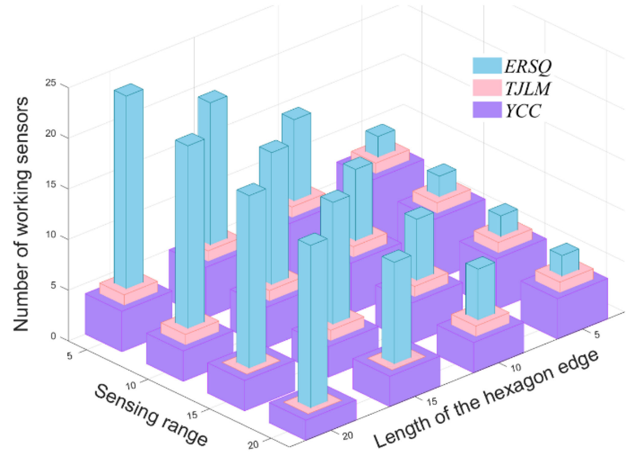

Fig. 10. Comparison of three algorithms in terms of the number of working sensors.

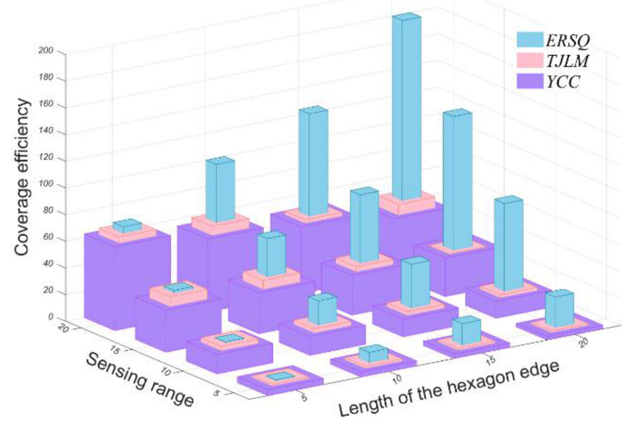

Fig. 11. Comparison of three algorithms in terms of the coverage efficiency.

from the *BS* will not be considered as the working sensors. As a result, the mobile charger will precharge the hexagon grid, which has a high impact on the connectivity, aiming to increase the number of working sensors.

Fig. 11 further compares the three algorithms in terms of the coverage efficiency, which is measured by the increased coverage divided by the move length of the mobile charger. A common trend of the three algorithms is that the coverage efficiency is increased with the sensing range. This occurs because that the recharged sensors have larger contributions to the coverage when the sensing range is increased. On the other hand, the increase of the length of the hexagon edge can enlarge the hexagon size and, hence, include more sensors. Since the mobile charger can recharge all the sensors in the hexagon at the same time, more sensors will be recharged, increasing the coverage efficiency. In comparison, the proposed ERSQ algorithm can recharge more sensors with a smaller movement distance, leading to a larger coverage efficiency, as compared with the other two related studies.

Fig. 12 compares the three algorithms in terms of the recharging efficiency, which is measured by the average number of recharged sensors divided by the move length of the mobile charger. The number of sensors varies ranging from 50 to 80

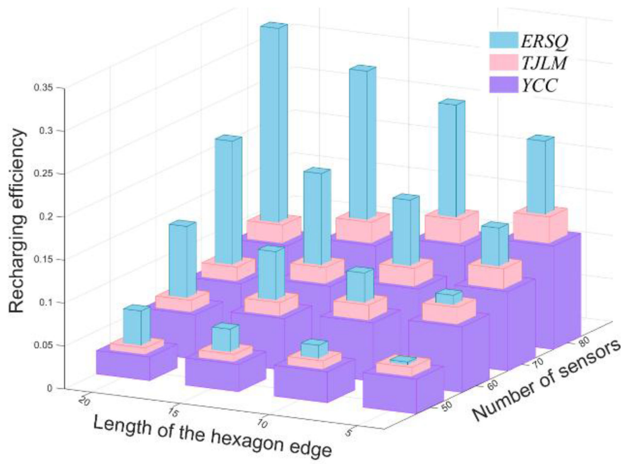

Fig. 12. Comparison of three algorithms in terms of the recharging efficiency.

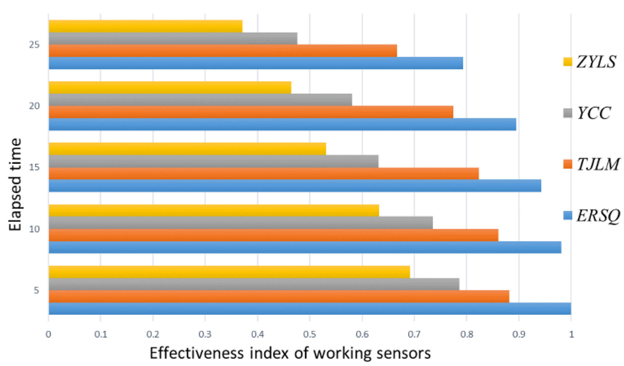

Fig. 13. Comparison of four algorithms in terms of the effectiveness index of working sensors.

while the length of the hexagon edge varies ranging from 5 to 20 m. The elapsed time is set at 50 time units and the sensing range of each sensor is set at 10 m. A common trend of the three algorithms is that the recharging efficiency is increased with the number of sensors deployed in the monitoring region. This occurs because that a larger number of deployed sensors can increase the number of sensors in each hexagon grid. This leads to the situation that the number of sensors to be simultaneously recharged is increased. In comparison, the proposed ERSQ algorithm outperforms the other two algorithms. This occurs because that the proposed ERSQ algorithm further considers the movement cost, coverage contribution as well as connectivity contribution.

Fig. 13 further compares the four algorithms in terms of the effectiveness index of working sensors. The effectiveness index of working sensors is defined as the ratio of the number of effective working sensors, which are working and connecting to the *BS* to the number of working sensors. The number of sensors is set at 50 while the length of the hexagon edge is set at 10 m. The elapsed time varies ranging from 5 to 25 time units. A common trend of the four algorithms is that the effectiveness index of working sensors is decreased with the elapsed time. This occurs because that the number of sleeping sensors is increased with the elapsed time due to energy consumptions, which leads to some working sensors being unable to connect to *BS*. As a result, the contributions of the disconnected working sensors cannot be counted. In comparison, the proposed ERSQ algorithm outperforms the other algorithms. This occurs because that the proposed ERSQ algorithm further considers the coverage contribution as well as the connectivity contribution.

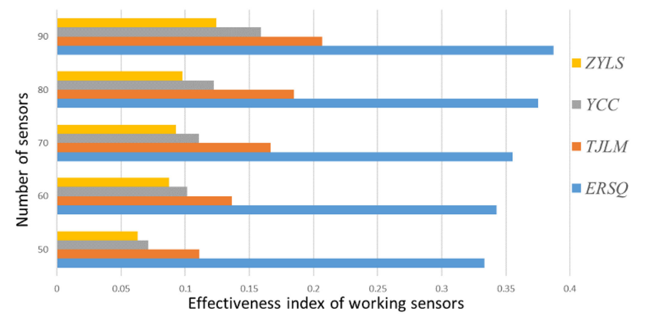

Fig. 14. Comparison of four algorithms in terms of the effectiveness index of working sensors.

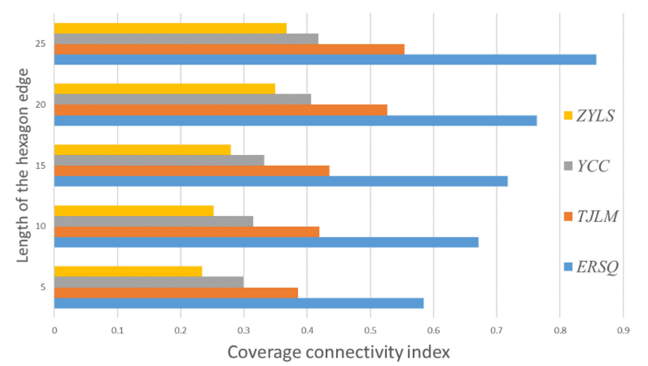

Fig. 15. Comparison of four algorithms in terms of the coverage connectivity index.

Fig. 14 further compares the four algorithms in terms of the effectiveness index of working sensors. The number of sensors is ranging from 50 to 90. The sensing range of each sensor is set at 10 m. The elapsed time is set at 50 time units. A common trend of the four algorithms is that their effectiveness indices of working sensors are increased with the number of sensors. This occurs because that each hexagon grid can include more sensors, which reduces the sleeping probability of each hexagon grid. This helps enlarge the number of working sensors connecting to the *BS*. In comparison, the proposed ERSQ algorithm outperforms the other algorithms. This occurs because that the proposed ERSQ algorithm further considers the connectivity contribution of the sensors in each hexagon grid.

Fig. 15 further compares the four algorithms in terms of the coverage connectivity index, which is defined as the ratio of the total coverage of the working and connected sensors to the total coverage of the working sensors. The number of sensors is set at 50 while the observation time is set at 50 time units. The length of the hexagon edge varies ranging from 5 to 25 m. A common trend of the four algorithms is that their coverage connectivity indices are increased with the length of the hexagon edge. This occurs because that the number of sensors included in each hexagon grid is increased. The increase of the edge length of the hexagon can enlarge the number of sensors to be

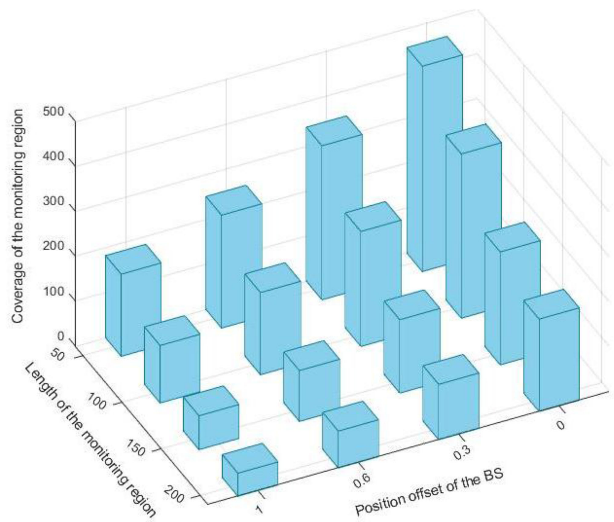

Fig. 16. Comparison of the ERSQ algorithm in terms of the coverage of the monitoring region.

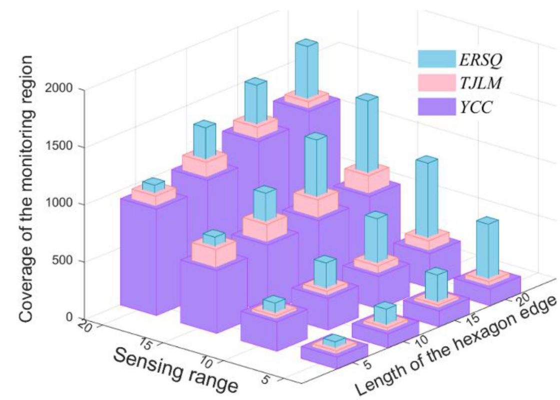

Fig. 17. Comparison of three algorithms in terms of the coverage of the monitoring region in the same situations.

included in it and finally increase the number of working sensors. Furthermore, it enlarges the number of sensors connecting to the *BS*, leading to a larger contribution. In comparison, the proposed ERSQ algorithm outperforms the other algorithms. This occurs because that the proposed ERSQ algorithm further considers the coverage contribution as well as the connectivity contribution.

Fig. 16 compares the proposed algorithms in terms of coverage by varying the length of the monitoring region ranging from 50 to 200 m and the position offset of the *BS* ranging from 0 to 1. The position offset of the *BS* is defined as the ratio of the distance between the position of the *BS* and the center of the monitoring region to the distance from the center of the monitoring region to the edge. The length of the hexagon edge is set at 20 m while the sensing range of each sensor is set at 5 m. The number of sensors is set at 90 and the elapsed time is set at 5 units. A common trend of the algorithms is that the coverages are decreased with the length of the monitoring region and the position offset of the *BS*. This occurs because that when the length of the monitoring region increases, the monitoring region has a lower probability to be covered by the sensing range leading to a decrease in the coverage ratio. In addition, the moving cost of the mobile charger increases leading to an increase of sleeping sensors' number due to the exhaustion of their energies, resulting in coverage loss. As *BS* moves from the center of the monitoring region to the edge, the importance of the connectivity increases leading to the more uneven energy consumption of the sensors. On the other hand, the mobile charger starts from the *BS* to charge the sensor that needs to be charged, so the position offset of the *BS* will increase the moving cost of the mobile charger and reduce the probability of the sensor being charged. As a result, the number of sleeping sensors due to the exhaustion of their energies increases, resulting in a decrease in the coverage of the monitoring region.

Fig. 17 compares the three algorithms in terms of coverage by varying the length of the hexagon edge and the sensing range of sensors. The number of sensors is set at 25 while the elapsed time is set at 50 time units. The three algorithms are in the same situation, i.e., the mobile charger will charge all the sensors in each grid at the same time. The proposed ERSQ algorithm removes the contribution of network connectivity. A common trend of the three algorithms is that their coverages are increased with both the sensing range and the length of the hexagon. When the sensing range of each sensor is increased, its covered area is also increased, which helps increase the coverage contribution. As a result, the coverages of the three algorithms are increased with the sensing range. In addition, the moving cost of the mobile charger decreases with the increase of the hexagon edge. As a result, the probability of the sensors in each hexagon grid being recharged is increased. In comparison, the performance of the proposed ERSQ algorithm is better than those of the other algorithms. This occurs because the proposed ERSQ algorithm takes into consideration the coverage contribution in (14) and gives priority to recharging the one with improved coverage.

VI. Conclusion

Energy recharging using a mobile charger is an important issue that has received much attention in recent years. However, most existing studies considered the distance between and requested sensors and the mobile charger and the emergencies of the requested sensors. This article proposes an ERSQ algorithm aiming to maximize the surveillance quality using a mobile charger in WSNs. Compared with the existing studies, this article additionally considers the coverage and connectivity benefits since the main purpose of energy recharging is to provide the highest surveillance quality. The proposed ERSQ algorithm mainly consists of two phases. The *initial phase* partitions the monitoring region into several regular hexagon grids and establishes the coordinate system for the grids. Then the CBBE phase further calculates the benefit of each hexagon grid based on its coverage and connectivity contributions. Performance study shows that the proposed ERSQ outperforms the existing studies in all cases in terms of surveillance quality and recharging efficiency. Future work will further develop distributed recharging algorithm and consider the cooperation of multiple mobile chargers.

References

[1] C. Chang, C. Lin, C. Shang, I. Chang, and D. Roy, "DBDC: A distributed bus-based data collection mechanism for maximizing throughput and lifetime in WSNs," *IEEE Access*, vol. 7, pp. 160506–160522, Oct. 2019.

[2] P. Xu, J. Wu, C. Shang, and C. Chang, "GSMS: A barrier coverage algorithm for joint surveillance quality and network lifetime in WSNs," *IEEE Access*, vol. 7, pp. 159608–159621, Oct. 2019.

[3] X. Ren, W. Liang, and W. Xu, "Data collection maximization in renewable sensor networks via time-slot scheduling," *IEEE Trans. Comput.*, vol. 64, no. 7, pp. 1870–1883, Jul. 2015.

[4] A. Kansal, J. Hsu, S. Zahedi, and M. Srivastava, "Power management in energy harvesting sensor networks," *ACM Trans. Embedded Comput. Syst.*, vol. 6, no. 4, pp. 32–69, Sep. 2007.

[5] W. Xu, W. Liang, X. Jia, Z. Xu, Z. Li, and Y. Liu, "Maximizing sensor lifetime with the minimal service cost of a mobile charger in wireless sensor networks," *IEEE Trans. Mobile Comput.*, vol. 17, no. 11, pp. 2564–2577, Nov. 2018.

[6] C. Wang, J. Li, Y. Yang, and F. Ye, "A hybrid framework combining solar energy harvesting and wireless charging for wireless sensor networks," in *Proc. IEEE INFOCOM 35th Annu. IEEE Int. Conf. Comput. Commun.*, 2016, pp. 1–9.

[7] A. Kurs, A. Karalis, R. Moffatt, J. Joannopoulos, P. Fisher, and M. Soljačić, "Wireless power transfer via strongly coupled magnetic resonances," *Science*, vol. 317, no. 5834, pp. 83–84, Jul 2007.

[8] G. Chen *et al.*, "A greedy constructing tree algorithm for shortest path in perpetual wireless recharging wireless sensor network," *J. Supercomput.*, vol. 75, no. 9, pp. 5930–5945, Jun. 2019.

[9] A. Kurs, R. Moffatt, and M. Soljačić, "Simultaneous mid-range power transfer to multiple devices," *Appl. Phys. Lett.*, vol. 96, no. 4, pp. 44102–44104, Jan. 2010.

[10] A. Mohamed, "Optimizing the performance of wireless rechargeable sensor networks," *IOSR J. Comput. Eng.*, vol. 19, no. 4, pp. 61–69, Sep. 2017.

[11] H. Yu, G. Chen, S. Zhao, C. Chang, and Y. Chin, "An efficient wireless recharging mechanism for achieving perpetual lifetime of wireless sensor networks," *Sensors*, vol. 17, no. 1, pp. 13–34, Dec. 2016.

[12] J. Zhu, H. Yu, Z. Lin, N. Liu, H. Sun, and M. Liu, "Efficient actuator failure avoidance mobile charging for wireless sensor and actuator networks," *IEEE Access*, vol. 7, pp. 104197–104209, Jul. 2019.

[13] W. Tu, X. Xu, T. Ye, and Z. Cheng, "A study on wireless charging for prolonging the lifetime of wireless sensor networks," *Sensors*, vol. 17, no. 7, pp. 1560–1573, Jul. 2017.

[14] B. Liu, N. Nguyen, V. Pham, and Y. Lin, "Novel methods for energy charging and data collection in wireless rechargeable sensor networks," *Int. J. Commun. Syst.*, vol. 30, no. 5, pp. 3050–3059, Sep. 2015.

[15] M. Tian, W. Jiao, J. Liu, and S. Ma, "A charging algorithm for the wireless rechargeable sensor network with imperfect charging channel and finite energy storage," *Sensors*, vol. 19, no. 18, pp. 3887–3905, Sep. 2019.

[16] S. Alkhalidi, D. Wang, and Z. Al-Marhabi, "Sector-based charging schedule in rechargeable wireless sensor networks," *KSII Trans. Internet Inf. Syst.*, vol. 11, no. 9, pp. 4301–4319, Sep. 2017.

[17] W Wen, C. Chang, S Zhao, and C. Shang, "Cooperative data collection mechanism using multiple mobile sinks in wireless sensor networks," *Sensors*, vol. 18, no. 8, pp. 2627–2646, Aug. 2018.

[18] K. Rabkh, S. Ismail, M. Al-Shurman, I. Jafar, E. Alkhader, and M. Al-Mistarihi, "Performance evaluation of selective and adaptive heads clustering algorithms over wireless sensor networks," *J. Netw. Comput. Appl.*, vol. 35, no. 6, pp. 2068–2080, Nov. 2012.

[19] K. Darabkh, J. Zomot, and Z. Al-Qudah, "EDB-CHS-BOF: Energy and distance based cluster head selection with balanced objective function protocol," *IET Commun.*, vol. 13, no. 19, pp. 3168–3180, Aug. 2019.

Yuanping Kan received the M.S. degree in science from Wuhan University of Technology Wuhan, China, in 2006. He is currently working toward a Ph.D. degree in computer science and information engineering at Tamkang University, New Taipei, Taiwan.

He is currently a Full Lecturer with the School of Big Data and Artificial Intelligence, Fujian Polytechnic Normal University, Fuqing, China. His current research interests include information security, Internet of Things, wireless sensor networks, and artificial intelligence.

Chih-Yung Chang (Member, IEEE) received the Ph.D. degree in computer science and information engineering from the National Central University, Taoyuan City, Taiwan, in 1995.

He is currently a Distinguish Professor with the Department of Computer Science and Information Engineering, Tamkang University, New Taipei, Taiwan. His current research interests include Artificial Intelligence, Internet of Things, wireless sensor networks, and smart healthcare.

Prof. Chang was an Associate Guest Editor for several SCI-indexed journals, including *International Journal of Ad Hoc and Ubiquitous Computing* from 2011 to 2021, *International Journal of Distributed Sensor Networks* from 2012 to 2014, *IET Communications* in 2011, *Telecommunication Systems* (TS) in 2010, *Journal of Information Science and Engineering* in 2008, and *Journal of Internet Technology* from 2004 to 2008.

Chin-Hwa Kuo received the B.S. degree in mechanical engineering from Chung-Yuan University, Taoyuan City, Taiwan, in 1980, the M.S. degree in electrical engineering from Marquette University, Milwaukee, WI, USA, in 1989, and the Ph.D. degree in electrical engineering from the University of Notre Dame, South Bend, IN, USA, in 1994.

He is currently a Full Professor with the Department of Computer Science and Information Engineering, and Chief of Information Officer, both with Tamkang University, Taipei, Taiwan. His research interests include multimedia processing and applications, learning analytics, and large-scale deployment of information communications technology in education.

Diptendu Sinha Roy received the Ph.D. degree in engineering from Birla Institute of Technology, Mesra, India, in 2010.

In 2016, he was with the Department of Computer Science and Engineering, National Institute of Technology (NIT) Meghalaya, Shillong, India as an Associate Professor, where he has been the Chair of the Department of Computer Science and Engineering since January 2017. Prior to his stint with National Institute of Technology, Meghalaya, he had served with the Department of Computer science and Engineering, National Institute of Science and Technology, Berhampur, India. His current research interests include software reliability, Distributed and Cloud Computing, and Internet of Things, specifically applications of artificial intelligence/Machine Learning for smart integrated systems.

Dr. Sinha Roy is a member of the IEEE Computer Society.